

Bird and micro-drone spectral width and classification

White, Daniel; Jahangir, Mohammed; Wayman, Joseph P. ; Reynolds, Jim; Sadler, Jon; Antoniou, Michail

DOI:

[10.23919/IRS57608.2023.10172408](https://doi.org/10.23919/IRS57608.2023.10172408)

License:

Other (please specify with Rights Statement)

Document Version

Peer reviewed version

Citation for published version (Harvard):

White, D, Jahangir, M, Wayman, JP, Reynolds, J, Sadler, J & Antoniou, M 2023, Bird and micro-drone spectral width and classification. in *2023 24th International Radar Symposium (IRS)*. Proceedings International Radar Symposium, IEEE, International Radar Symposium IRS 2023, Berlin, Germany, 24/05/23. <https://doi.org/10.23919/IRS57608.2023.10172408>

[Link to publication on Research at Birmingham portal](#)

Publisher Rights Statement:

D. White, M. Jahangir, J. P. Wayman, S. J. Reynolds, J. P. Sadler and M. Antoniou, "Bird and Micro-Drone Doppler Spectral Width and Classification," 2023 24th International Radar Symposium (IRS), Berlin, Germany, 2023, pp. 1-10, doi: 10.23919/IRS57608.2023.10172408.

© 2022 IEEE. Personal use of this material is permitted. Permission from IEEE must be obtained for all other uses, in any current or future media, including reprinting/republishing this material for advertising or promotional purposes, creating new collective works, for resale or redistribution to servers or lists, or reuse of any copyrighted component of this work in other works.

General rights

Unless a licence is specified above, all rights (including copyright and moral rights) in this document are retained by the authors and/or the copyright holders. The express permission of the copyright holder must be obtained for any use of this material other than for purposes permitted by law.

- Users may freely distribute the URL that is used to identify this publication.
- Users may download and/or print one copy of the publication from the University of Birmingham research portal for the purpose of private study or non-commercial research.
- User may use extracts from the document in line with the concept of 'fair dealing' under the Copyright, Designs and Patents Act 1988 (?)
- Users may not further distribute the material nor use it for the purposes of commercial gain.

Where a licence is displayed above, please note the terms and conditions of the licence govern your use of this document.

When citing, please reference the published version.

Take down policy

While the University of Birmingham exercises care and attention in making items available there are rare occasions when an item has been uploaded in error or has been deemed to be commercially or otherwise sensitive.

If you believe that this is the case for this document, please contact UBIRA@lists.bham.ac.uk providing details and we will remove access to the work immediately and investigate.

Bird and Micro-Drone Doppler Spectral Width and Classification

Daniel White, Mohammed Jahangir, Joseph P. Wayman,
S. James Reynolds, Jon P. Sadler, Michail Antoniou

University of Birmingham
Birmingham, United Kingdom

email: {d.white.4, m.jahangir, j.wayman, j.reynolds.2, j.p.sadler, m.antoniou}@bham.ac.uk

***Abstract:** This paper reports on the class separability of spectrograms featuring bird and micro-drone targets produced by an L-Band staring radar. Multi-rotor drones with small propellor blades are less likely to show strong micro-Doppler sidebands depending on the range and operating frequency. With this, we were incentivized to measure the separability of the target classes relying only on the body Doppler information captured in the spectrograms. A spectral width feature extraction method was tested using both a set of single drone and bird targets, as well as a larger dataset including spectrograms containing multiple targets and a mixture of classes. These features were employed to inform a simple classifier yielding an 83% classification accuracy in the single target case. The results were then compared to a convolutional neural network baseline that achieved 89% accuracy on the larger, more complex dataset.*

1. Introduction

The prevalence of, and risk of damage or injury from, drones is ever-increasing [1]. The need for surveillance systems to detect, track and classify an arbitrary airborne target can be achieved with a range of solutions [2], including radar. Radar is an optimal tool for detection as it allows for 24hr operation, and its design can be tailored to suit any operational scenario (maximum detection range, field of regard, effect of weather), budget constraints notwithstanding [3], [4]. Developments in simultaneously deployed networked radars are ongoing [5]-[7] and promise ubiquitous low-cost surveillance of an airspace. Staring radars [3] and multiple-input-multiple-output systems [8] allow for the simultaneous tracking of numerous targets. Classification of drone targets is made challenging by the existence of birds that are of similar size and occupy the airspace with similar flight characteristics. Radar surveillance systems detect these confuser targets but the confidence of automatic classification methods will diminish at the extremes of the system's operational performance.

Micro-Doppler modulations from the movement of large drones' propellor blades can be detected alongside the main body motion in radar systems [9],[10]. This is an important differentiating feature as micro-Doppler from birds is much reduced compared with that of drones at low frequencies [11], [12], and is sufficiently differentiable at higher frequencies [13], [14]. Research has demonstrated that the classification of drones with the presence of micro-Doppler returns is a challenge met by current approaches [15]-[17], but at low frequencies and at long ranges, small drones with small propellor blades may not produce detectable micro-Doppler. This leads to bird presence yielding higher rates of false positives and missed drones that possess no measurable micro-Doppler [18]. Classification in this instance is more difficult, which is a concern as smaller drones are cheaper, are more easily concealed and are highly available with a more active second-hand market due to their great appeal to consumers compared to expensive, large, heavy drone systems. This paper presents spectrograms collected of bird and micro-Doppler-less small drone targets and explores how a key feature of the target's



spectral width may support their classification alongside results from a Convolutional Neural Network (CNN) applied to the same dataset. The remainder of this paper is organized as follows: Section 2 details the radar, environment, drone targets and opportune birds collected and analyzed in the following sections. Section 3 presents the results of body Doppler width extracted from the dataset and class separation is measured using this feature. Section 4 shows the classification performance on the dataset when using a CNN. Section 5 compares the efficacy of these methods within the parameters of the radar and its environment. Finally, Section 6 draws conclusions.

2. Experimental Dataset

The University of Birmingham has installed two staring radars on its Edgbaston campus. These commercial off-the-shelf L-Band systems have a maximum instrumented range of 10 km and operate with a 90° azimuth and 60° elevation sector. These systems have a large Doppler resolution enabled by a high pulse repetition frequency and continuous integration of returns through its staring nature. The radar used in this study is directed towards the Birmingham city centre, across urban and suburban areas, making it a difficult operational environment due to the effects of strong clutter that can potentially suppress detection of slow moving, low, observable targets. More details of the radars and the facility can be found in [19]. The staring radar divides the field of view into resolution cells in range, azimuth and elevation. The receive beams of the staring radar are broad in azimuth and elevation, and so collected opportune bird spectrograms frequently feature returns of many targets that may not be co-located. Likewise, the collected drone signatures frequently show presence of bird targets that have encroached into the resolution cell of the target during its flight. A spectrogram is formed from a target’s positional track by concatenating the Doppler returns of the resolution cell measured to contain the target for all points of the track. A short-time Fourier transform is applied over the collected timeseries returns resulting in a 2D spectrogram image. The spectrograms reported in this paper were produced using a Coherent Processing Interval (CPI) consisting of 4,096 pulses with Blackman-Harris window and a 50% overlap of successive CPIs [20]. Each CPI lasts 280 ms and the spectrogram update rate is 3.7 Hz.

Drone trials have routinely taken place since the 2021 installation of the radar with a variety of quadcopter models. Two popular, small DJI drone models were used in this study and their specifications are provided in Table 1. The drones were flown in a controlled and repeatable manner; they took off from a point in the radar view and reached a predetermined altitude above the ground (either 60, 80 or 100 m). Various loops of different shapes and sizes were then flown. For repeated flight patterns, the drones were operated with different speed modes selected (cinematic, normal and sport) to increase the variability of collected returns in the dataset. Each drone track was cropped to a time window when the drone was at mission height and had a radial velocity greater than a threshold of 0.01 m/s to ensure consistent presence of a detectable drone in the data.

Table 1 – Drones Targets Used in Classification Study

Target	Mass (g)	Body Diagonal (mm)	Blade Radius (mm)	Price (~£1,000)	Image
DJI Mini 2	249	213	60	0.3	
DJI Mavic 3	895	400	110	0.6	

The flights of the birds within the radar field of view of the Birmingham area are constantly observed and tracked by the radar. Opportune bird spectrograms were formed by extracting the resolution cells containing the target over the course of its flight. With the absence of labelling of these targets, efforts were required to ensure collected data originated from birds. Tracks over the radar’s recording period were collected and filtered to have duration greater than 38 seconds and have a mean height above the radar. All remaining tracks had their spectrograms produced and visually labelled by the authors to whether they were unambiguous examples of bird targets suitable for comparison against a drone flight. During this step, bird spectrograms were labelled if they were instances of a single target only being tracked, compared to if multiple birds were in close proximity to each other in the same resolution cell. Drone targets were also treated this way and each flight was labelled if birds had encroached into the drone spectrogram. Figure 1 shows the positions of collected targets in the single target and all targets datasets. All but three drone flights were performed less than 2 km from the radar, whilst birds were present over the radar’s field of view. Figure 2a-d shows representative examples of bird and drone targets both with and without presence of other nearby but separate targets.

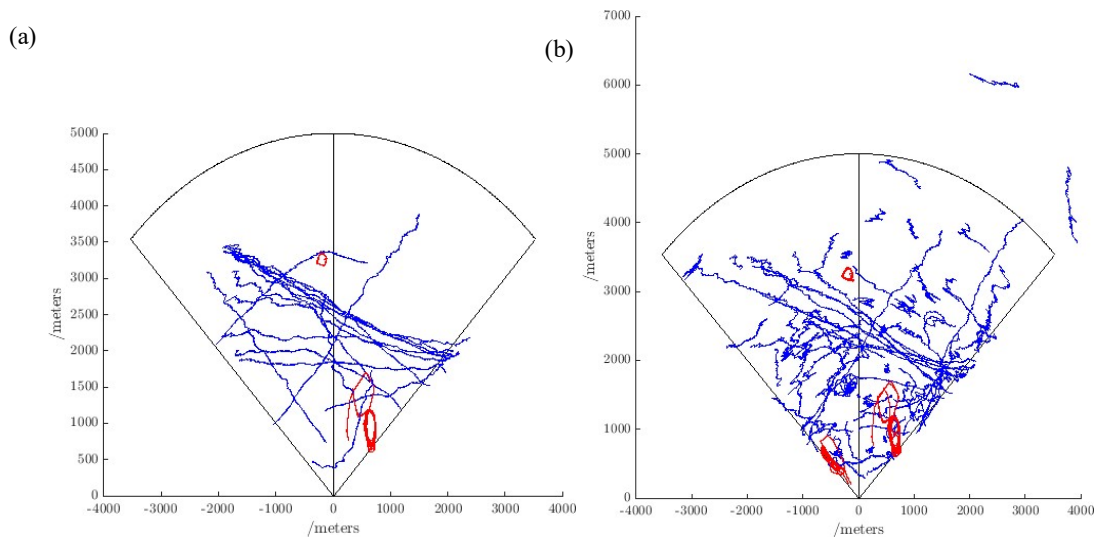


Figure 1. Coverage of (a) single and (b) all targets considered in the datasets. Targets are either drones (red) or birds (blue).

The receive beams of the staring radar used were broad in azimuth and elevation. Collected opportune bird spectrograms frequently featured returns of many targets that may not have been co-located. Likewise, the collected drone signatures frequently revealed presence of bird targets that had encroached into the resolution cell of the target during its flight. Figure 3a-d below show representative examples of single bird and drone targets both with and without presence of other nearby but separate targets. Figures 2c and d show examples of numerous birds present in an area. Figure 2c shows that our smallest drone was not always the strongest target present and so presents a very difficult challenge for a classifier. From the collected bird and drone signatures, two datasets were assembled of single targets and all targets. The single target dataset was a set of targets where each entry was verified to contain infrequent, low Signal-to-Noise Ratio (SNR) presence of other nearby targets. The quantities of the classes in the datasets are shown in Table 2 broken down into number of flights and total number of frames per flight.

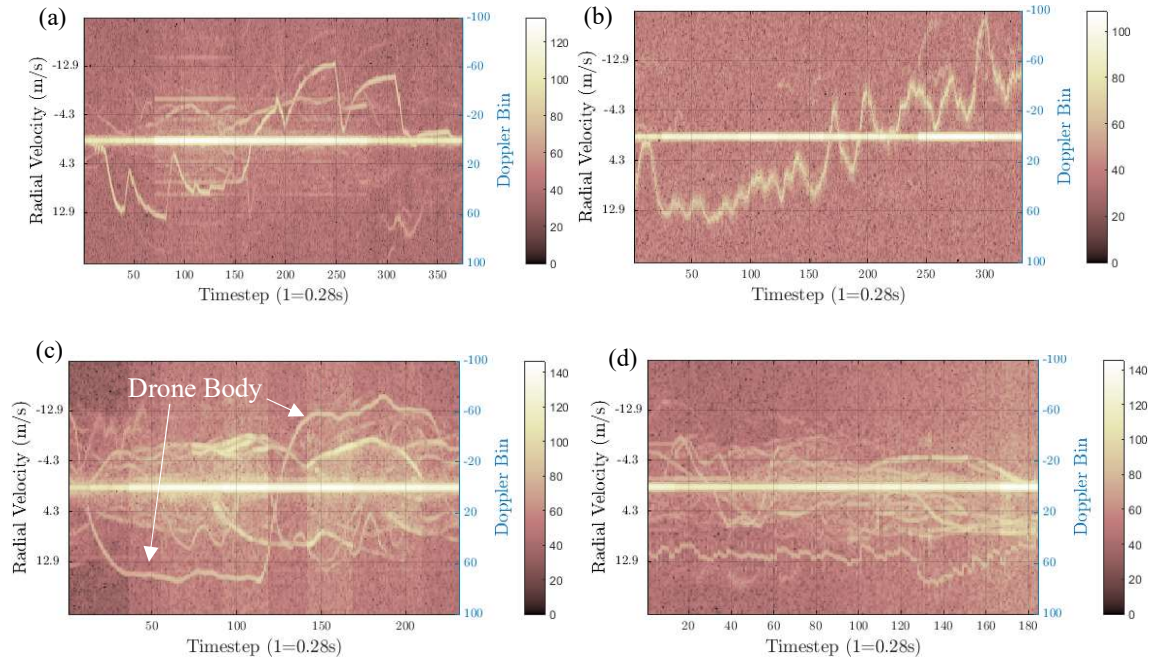


Figure 2. Example spectrograms of collected targets in the dataset, of (a) DJI Mavic 3, (b) a single opportune bird, (c) DJI Mini 2 with presence of nearby birds, and (d) multiple opportune birds.

Table 2 – Quantities of targets in the datasets used for feature analysis.

Target	Single Birds	Single Drones	All Birds	All Drones
# Flights	35	10	64	95
# Frames	10,034	9,127	27,059	27,416

3. Body Width Extraction

This section will describe the simple method of body width extraction and the class separability of results from a derived feature set. Basic body width statistics were derived over different temporal windows of the target’s track, and a 4D k-Nearest Neighbors algorithm (kNN) was applied to the body width features that best separated the targets classes when applied to the whole dataset.

3.1 Body Width Feature Extracting

The method for body width feature extracting began with finding the Doppler bin with peak SNR for each frame in the spectrogram, ignoring the main clutter peak. Extending left and right of this peak, the body width was defined by setting a threshold at mean noise power + 5dB and marking the furthest Doppler bin from the body peak where the signal power was above this threshold. These points are illustrated with an example spectrum in Figure 3a. An example of the body width measurement is presented with the source spectrogram in Figure 3b.

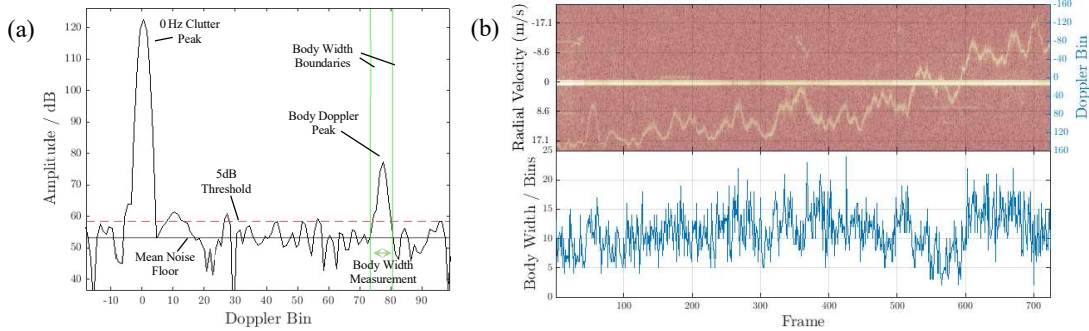


Figure 3a-b. Body Width Extraction

- (a) Body width calculated from the Doppler spectrum of a single DJI Mavic 3 frame
- (b) Body width feature value of example bird spectrogram.

As well as the width at each point being measured, the degree and nature of the fluctuation of this value were compared using three metrics over three different temporal windows - the average, the range of and the standard deviation over 5, 15 and 45 frames, corresponding to 1.3, 4.1 and 12.2 seconds of real time, respectively. The range was the number of Doppler bins between the highest and lowest values measured in the time window. The thickness of the peak for a small drone was usually smaller than and more constant across the flight than most birds, an example of which can be seen in Figure 2a in comparison with Figure 2b.

3.2 Separability of Classes with Body Width

Figure 4 shows histograms of class separability with probability scores of separation calculated using a logistical regression classifier [21] inllet to gauge numerically how naturally separable targets were using body width features. The single target case used 9,127 drone frames and an equal number of randomly sampled bird frames, whilst in the all targets set 27,059 samples per class were used. Bird returns were found to be thicker than drones in the single target case (Fig. 4a), but this degraded in the larger dataset of all targets (Fig. 4b). The logistic regression classification result is the lowest expected performance probability when using the body width feature alone. The top image in Figure 4 is the body width per frame, and the sub-rows are the mean, standard deviation and range, with sub-columns as these statistics calculated over 5, 15 and 45 frame windows. Using the mean of the body width improved the separation of targets in the single target case, and for the range and standard deviation features, the two longer windows improved the separation beyond the single frame body width separation measure. For the all target dataset, the level of class separation from these features was much lesser. The strongly overlapping histograms and classification probabilities close to 50% show that multiple targets

in the spectrogram have severely reduced the reliability of the body width feature for classification.

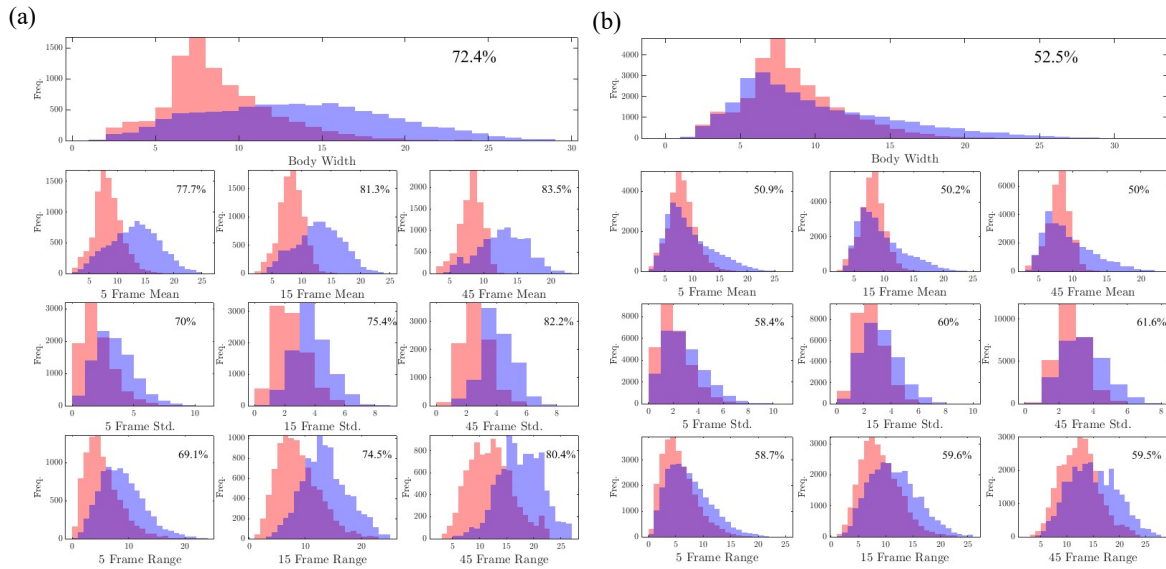


Figure 4. Histograms of body width measurements vs class. Distributions are of drones (red) and birds (blue). Number inlet is accuracy of logistic regression classifier. (a) Single Targets Only (b) All Targets.

The best performing feature from each row of Figure 4 was applied to a standardized kNN classifier to provide a baseline overall classification result and to investigate if features combined non-linearly to boost classification performance significantly. For the single target case, these were the longest, 45 frame windows. For the all target case, these were the 5 frame mean, the 45 frame standard deviation, and 15 frame range. For the single target case, the 4D kNN results shown in Figure 5a performed more poorly than the best 1D logistic regression classifier, showing that the feature sets were similar in their distribution amongst the samples in the dataset. For the all target dataset, the kNN classification result was better than that achieved from any of the logistic classifier results, indicating that the extracted features were less related to the genuine body width of targets and were susceptible to corruption in this current simple implementation.

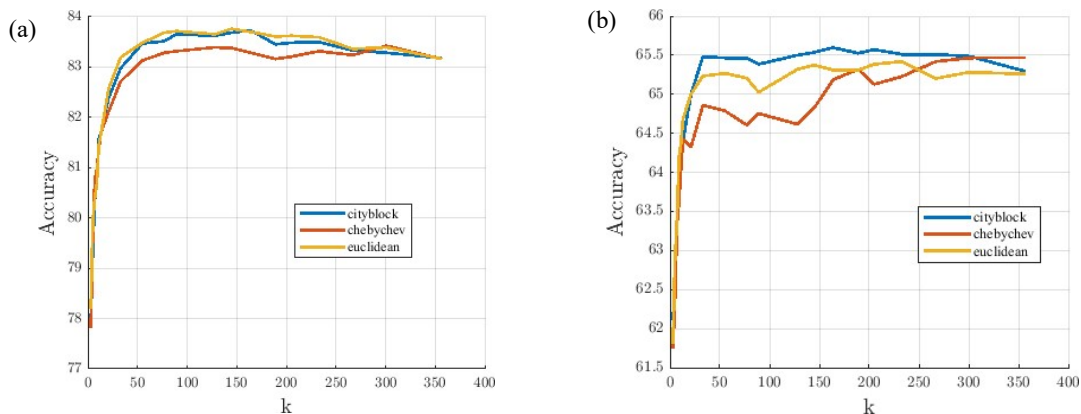


Figure 5. Standardized kNN performance for best performing body width features.
 (a) Single Targets: Body Width, 45 Frame Mean, 45 Frame Standard Deviation, 45 Frame Range.
 (b) All Targets: Body Width, 5 Frame Mean, 45 Frame Standard Deviation, 15 Frame Range.

4. Automatic Feature Extraction

Convolutional Neural Networks [22] are a type of deep learning classifier that learns features of input data from a training cycle in convolutional layers and predicts a class from the features through a dense series layer. Abstract features relevant to common patterns can be provided in abundance through the use of pretrained classifiers that achieve excellent performance on large, highly varied external datasets [23]. In this study, only the fully connected layers were retrained for bird and drone targets. The large CNN model ‘Alexnet’ [24] was used as it has been shown to maintain its performance as the SNR of a dataset decreases compared to alternatives [25] which is paramount for a reliable classification across the range of possible target occurrences. Table 3 shows the quantities of training, testing and validation data used in the training process. The input images were formed of 20 frames of the spectrogram each corresponding to ~5.5 seconds of dwell time. Red-green-blue images were used for this analysis to accommodate Alexnet’s 3-channel input layer. Training was stopped at the first occurrence of the maximum sum of training and validation scores calculated every epoch which is an effective way to predict the best test accuracy when using a large dataset. The Adam [26] optimizer was used with (squared) gradient decay factors of (0.999) 0.9 with 10^{-5} L2 Regularization and suitable training parameters were found with a grid search yielding an initial learn rate of 10^{-4} and mini-batch size of 32.

Table 3 – Summary of Data Quantities used for CNN Evaluation

Set	Targets	#Flights	#Images
Training	Bird	58	814
	Mini 2	26	654
	Mavic 3	9	153
	814 Birds	807 Drones	1621 Total
Testing	Bird	35	480
	Mini 2	17	317
	Mavic 3	10	160
	480 Birds	477 Drones	957 Total
Validation	Bird	2	29
	Mini 2	1	21
	Mavic 3	1	14
	29 Birds	35 Drones	63 Total

Training was repeated nine times with different initialization seeds and the median confusion matrix is presented in Figure 6 alongside a map of the location of classification results. The resultant accuracies ranged from 88.61 to 91.11% (mean: 89.16%, median: 89.24%), with a drone and bird recalls of 90.6% and 86.4%, respectively, where recall is the probability that a classification prediction is incorrect. There was a 4% increase in the false positives of bird detection rates, so this classifier was more susceptible to false alarm misclassifications than a missed detection.

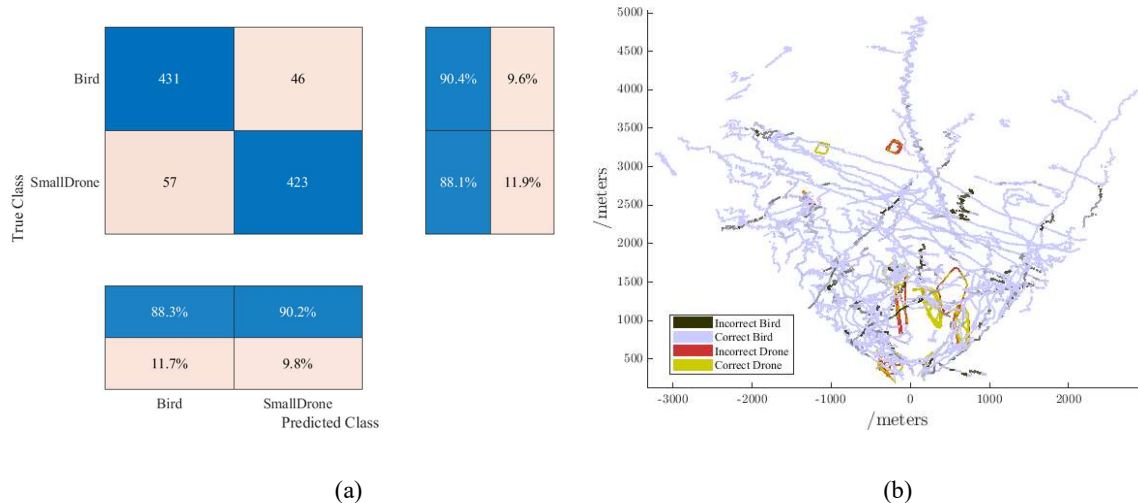


Figure 6. CNN classifier results of Bird and Drone targets.
(a) Median confusion matrix (b) Map of classified test set.

5. Results Comparison and Discussion

The CNN classifier performed well on the dataset of all targets, showing that the non-linear features extracted provided enough separability to inform the decision layers to a 90% accuracy benchmark. Previous similar studies using the CNN for bird-drone classification have shown similar high-performance benchmarks such as 93.56% classification for bird vs small and large drones in [17] and <92% for large drone vs bird classification in [24]. These studies that used the same radar system as this current study demonstrated that deep, machine learned classifiers are capable of classifying small drone and bird classes with a high-performance level. This current study is the first demonstration of differentiating smaller drone targets from birds and performance did not heavily deteriorate with the absence of micro-Doppler signatures. The body width extracted feature produced a classifier with ~82% accuracy when targets were ensured to be isolated in the spectrogram.

Extending the dataset to include mixed target spectrograms caused the body width feature classification to perform up to ~18% worse. Body width using the simple algorithm, explained in Section 3.1, was highly susceptible to corruption with the presence of multiple targets in the spectrogram, but overall results revealed that single drones had a thinner, less fluctuating spectral appearance than single birds. The drones used were at a closer range than the birds. Body thickness at increasing ranges will reduce with SNR, and as drones had on average a smaller body width we expect our findings to apply well at all ranges. Body width may prove to be an important feature for classification as it is a quantity that is always measurable in a detected target, and so it can provide a reasonable baseline feature for classification in concert with other features and classification approaches for radar systems with narrow beamwidths and smaller range resolutions. We expect this feature could be employed effectively in a hierarchical classifier, where it can be used upon failing to measure micro-Doppler returns from a detected target, for instance. Systems that cannot spatially resolve targets will need to rely on data-driven solutions to determine the presence of restricted drones amongst birds and other confuser objects.

6. Conclusions

This study is an introduction to the class separability of small drone and bird targets without the presence of rotor-induced micro-Doppler reported through an L-Band system. Body width was investigated as a differentiating feature and provided a reasonable 82% baseline of performance on single targets, but performance and discovered trends fell when spectrograms contained a mix of target classes. A CNN was trained to achieve 89-90% accuracy when tested on a large dataset containing both single and mixed targets, which was similar to the performance expected from datasets containing strong presence of large drone micro-Doppler. The University of Birmingham staring radar facility will continue to investigate the application of feature and deep learning for target classification. Future work will investigate the inclusion of tracker trajectory features and further spectral features including body width in comparison and in fusion with features and classification systems from deep learned data-driven methods.

Acknowledgements

Funded by the UK Government's Future Aviation Security Solutions (FASS) programme and its Industrial PhD Partnership initiative delivered by Connected Places Catapult. Thanks also to EPSRC MEFA (EP/T011068/1) and the UK National Quantum Technology Hub in Sensing and Timing (EP/T001046/1) projects for their support.

References

- [1] J. Wang, Y. Liu, and H. Song, "Counter-Unmanned Aircraft System(s) (C-UAS): State of the Art, Challenges, and Future Trends," *IEEE Aerospace and Electronic Systems Magazine*, vol. 36, no. 3, pp. 4–29, 2021.
- [2] B. Taha and A. Shoufan, "Machine Learning-Based Drone Detection and Classification: State-of-the-Art in Research," *IEEE Access*, vol. 7, pp. 138669–138682, 2019.
- [3] M. Jahangir and C. Baker, "Robust Detection of Micro-UAS Drones with L-Band 3-D Holographic Radar," in *2016 Sensor Signal Processing for Defence (SSPD)*, 2016, pp. 1-5.
- [4] S. Harman, "A comparison of staring radars with scanning radars for UAV detection: Introducing the Alarm™ staring radar," in *2015 European Radar Conference (EuRAD)*, 2015, pp. 185-188.
- [5] X. Guo, C. S. Ng, E. de Jong and A. B. Smits, "Concept of Distributed Radar System for mini-UAV Detection in Dense Urban Environment," in *2019 International Radar Conference (RADAR)*, 2019, pp. 1-4.
- [6] M. Ritchie, F. Fioranelli, H. Griffiths and B. Torvik, "Monostatic and bistatic radar measurements of birds and micro-drone," in *2016 IEEE Radar Conference (RadarConf)*, 2016, pp. 1-5.
- [7] R. Palamà, F. Fioranelli, M. Ritchie, M. Inggs, S. Lewis and H. Griffiths, "Measurements and discrimination of drones and birds with a multi-frequency multistatic radar system", *IET Radar Sonar Navigat.*, vol. 15, no. 8, pp. 841-852, 2021.
- [8] J. Klare, O. Biallowons and D. Cerutti-Maori, "UAV detection with MIMO radar," in *18th International Radar Symposium (IRS)*, 2017, pp. 1-8.
- [9] P. Klaer, A. Huang, P. Sévigny, S. Rajan, S. Pant, P. Patnaik, and B. Balaji, "An Investigation of Rotary Drone HERM Line Spectrum under Manoeuvring Conditions," *Sensors*, vol. 20, no. 20, p. 5940, 2020.
- [10] R. I. A. Harmanny, J. J. M. De Wit, and G. Prémel Cabic, "Radar micro-Doppler feature extraction using the spectrogram and the cepstrogram," in *2014 11th European Radar Conf.*, 2014, pp. 165-168.

- [11] P. Beasley, M. Ritchie, H. Griffiths, W. Miceli, M. Inggs, S. Lewis and B. Kahn, "Multistatic Radar Measurements of UAVs at X-band and L-band," in *2020 IEEE Radar Conference (RadarConf20)*, 2020, pp. 1-6.
- [12] D. White, M. Jahangir, M. Antoniou, C. Baker, J. Thiyagalingam, S. Harman and C. Bennett, "Multi-rotor Drone Micro-Doppler Simulation Incorporating Genuine Motor Speeds and Validation with L-band Staring Radar," in *2022 IEEE Radar Conference (RadarConf22)*, 2022, pp. 1-6.
- [13] S. Rahman and D. A. Robertson, "Radar micro-Doppler signatures of drones and birds at K-band and W-band", *Scientific reports*, vol. 8, no. 1, pp. 17396, 2018.
- [14] A. Karlsson, M. Jansson and M. Hämläinen, "Model-Aided Drone Classification Using Convolutional Neural Networks," in *2022 IEEE Radar Conference (RadarConf22)*, 2022, pp. 1-6.
- [15] C. Bennett, M. Jahangir, F. Fioranelli, B. I. Ahmad and J. L. Kerneć, "Use of Symmetrical Peak Extraction in Drone Micro-Doppler Classification for Staring Radar," in *2020 IEEE Radar Conference (RadarConf20)*, 2020, pp. 1-6.
- [16] S. Rahman and D. A. Robertson, "Classification of drones and birds using convolutional neural networks applied to radar micro-Doppler spectrogram images", *IET Radar Sonar Navigat.*, vol. 14, no. 5, pp. 653-661, 2020.
- [17] X. Ren, M. Jahangir, D. White, G. Atkinson, C. Baker, and M. Antoniou, "Estimating Physical Parameters from Multi-Rotor Drone Spectrograms," in *International Conference on Radar Systems (RADAR 2022)*, 2022, pp. 20-25.
- [18] H. Dale, M. Jahangir, C. J. Baker, M. Antoniou, S. Harman and B. I. Ahmad, "Convolutional Neural Networks for Robust Classification of Drones," in *2022 IEEE Radar Conference (RadarConf22)*, 2022, pp. 1-6.
- [19] M. Jahangir, G. M. Atkinson, D. White, X. Ren, J. P. Wayman, C. J. Baker, J. P. Sadler, J. S. Reynolds and M. Antoniou, "Networked Staring Radar Testbed for Urban Surveillance: Status and Preliminary Results," in *International Conference on Radar Systems (RADAR 2022)*, 2022, pp. 471-476.
- [20] D. Park, S. Lee, S. Park, and N. Kwak, "Radar-Spectrogram-Based UAV Classification Using Convolutional Neural Networks," *Sensors*, vol. 21, no. 1, pp. 210, 2020.
- [21] J. Lever, M. Krzywinski and N. Altman, "Logistic regression," *Nature Methods*, vol. 13, pp. 541–542, 2016.
- [22] L. Alzubaidi, J. Zhang, A. J. Humaidi, A. Al-Dujaili, Y. Duan, O. Al-Shamma, J. Santamaría, M. A. Fadhel, M. Al-Amidie and L. Farhan, "Review of deep learning: concepts, CNN architectures, challenges, applications, future directions," *J. Big Data* vol. 8, no. 53, 2021.
- [23] B. W. Tienin, C. Guolong and R. M. Esidang, "Comparative Ship Classification in Heterogeneous Dataset with Pre-trained Models," in *2022 IEEE Radar Conference (RadarConf22)*, 2022, pp. 1-6.
- [24] A. Krizhevsky, I. Sutskever and G. Hinton, "ImageNet Classification with Deep Convolutional Neural Networks," in *Neural Information Processing Systems*, vol. 25, 2017.
- [25] H. Dale, C. Baker, M. Antoniou, M. Jahangir, G. Atkinson and S. Harman, "SNR-dependent drone classification using convolutional neural networks," *IET Radar Sonar Navig.*, vol. 1, no. 16, pp. 22– 33, 2022.
- [26] D. P. Kingma and J. Ba, "Adam: A Method for Stochastic Optimization," arXiv:1412.6980, 2015.